

## RESEARCH ARTICLE

# Particle algorithms for animal movement modelling in receiver arrays

Edward Lavender<sup>1</sup>  | Andreas Scheidegger<sup>1</sup>  | Carlo Albert<sup>1</sup>  | Stanisław W. Biber<sup>2</sup>  |  
 Janine Illian<sup>3</sup>  | James Thorburn<sup>4,5</sup>  | Sophie Smout<sup>6</sup>  | Helen Moor<sup>1</sup> 

<sup>1</sup>Department of Systems Analysis, Integrated Assessment and Modelling, Eawag Swiss Federal Institute of Aquatic Science and Technology, Dübendorf, Switzerland; <sup>2</sup>School of Engineering Mathematics and Technology, University of Bristol, Bristol, UK; <sup>3</sup>School of Mathematics and Statistics, University of Glasgow, Glasgow, UK; <sup>4</sup>School of Applied Sciences, Edinburgh Napier University, Edinburgh, UK; <sup>5</sup>Centre for Conservation and Restoration Science, Edinburgh Napier University, Edinburgh, UK and <sup>6</sup>Scottish Oceans Institute, University of St Andrews, St Andrews, UK

**Correspondence**

Edward Lavender

Email: [edward.lavender@eawag.ch](mailto:edward.lavender@eawag.ch)**Funding information**

Department of Systems Analysis,  
 Integrated Assessment and Modelling,  
 Eawag Swiss Federal Institute of Aquatic  
 Science and Technology

**Handling Editor:** Aaron Ellison**Abstract**

1. Particle filters and smoothers are sequential Monte Carlo algorithms used to fit non-linear, non-Gaussian state-space models. These algorithms are well placed to fit process-oriented models to animal-tracking data, especially in receiver arrays, but to date they have received limited attention in the ecological literature.
2. We introduce a Bayesian filtering–smoothing algorithm that reconstructs individual movements and patterns of space use from animal-tracking data, with a focus on passive acoustic telemetry systems. Within a sound probabilistic framework, the methodology integrates the movement process and the observation processes of disparate datasets, while correctly representing uncertainty. In a simulation-based analysis, we compare the performance of our algorithm to the prevailing heuristic methods used to study movements and space use in passive acoustic telemetry systems and analyse algorithm sensitivity.
3. We find the particle smoothing methodology outperforms heuristic methods across the board. Particle-based maps represent simulated movements more accurately, even in dense receiver arrays, and are better suited to analyses of home ranges, residency and habitat preferences.
4. This study sets a new state-of-the-art for movement modelling in receiver arrays. Particle algorithms provide a robust, flexible and intuitive modelling framework with potential applications in many ecological settings.

**KEYWORDS**

animal tracking, movement ecology, passive acoustic telemetry, patten, state-space model, utilisation distribution

This is an open access article under the terms of the [Creative Commons Attribution](https://creativecommons.org/licenses/by/4.0/) License, which permits use, distribution and reproduction in any medium, provided the original work is properly cited.

© 2025 The Author(s). *Methods in Ecology and Evolution* published by John Wiley & Sons Ltd on behalf of British Ecological Society.

## 1 | INTRODUCTION

Animal movement shapes ecological processes across biological scales (Nathan et al., 2008, 2022). Individual movements reflect behaviour, such as foraging (Shaw, 2020), social interactions (Jacoby & Freeman, 2016) and habitat preferences (Abrahms et al., 2021). Individual movements also underlie emergent patterns of space use that shape population dynamics (Morales et al., 2010), ecosystem functioning (Riotte-Lambert & Matthiopoulos, 2020) and interactions with humans (Rutz et al., 2020).

Technologies for animal tracking have advanced dramatically in recent decades (Nathan et al., 2022). Some technologies, such as satellite transmitters, record individual locations (or proxies thereof) through time. Others, such as passive acoustic telemetry, depend on receiver arrays that record detections when animals move within range (Matley et al., 2022). These are important solutions for animal tracking, especially in aquatic ecosystems where satellite tracking is limited (Hussey et al., 2015).

Passive acoustic telemetry is widely used to study the movements of aquatic animals (Matley et al., 2022; Whoriskey et al., 2019). This technology comprises acoustic receivers that listen continuously for individual-specific acoustic transmissions from tagged animals. When animals move within receiver detection ranges, detections may be recorded (depending on transmission distance and other variables) (Kessel et al., 2014). Unfortunately, receiver detection ranges are typically non-overlapping, resulting in detection gaps when animal locations are less certain. However, additional devices (such as archival depth tags) may continue to collect data during this time (Matley et al., 2023).

In passive acoustic telemetry systems, individual movements and patterns of space use are most commonly analysed with heuristic approaches (Kraft et al., 2023). The predominant method (the 'COA algorithm') takes weighted averages of the receiver locations where detections were recorded as 'relocations' for utilisation distribution (UD) estimation (Simpfendorfer et al., 2002; Udyawer et al., 2018). Other approaches treat the receiver array as a network, with nodes defined by receivers and edges defined by sequential detections. For example, the RSP methodology smooths interpolated 'relocations' along the shortest paths between receivers (Niella et al., 2020). However, there remains little research on how well heuristic methods represent patterns of space use (i.e. method 'performance') and the circumstances in which they can be usefully applied (Lavender et al., 2023).

Recent studies have encouraged a more process-orientated perspective that encapsulates the movement and measurement processes that generate observations (Hostetter & Royle, 2020; Lavender et al., 2023; Whoriskey et al., 2019). State-space models formalise this perspective by coupling a process model of the unobserved movement process to an observation model of the measurement process that connects movements to observations (Patterson et al., 2008). Yet fitting state-space models is challenging. In the case of satellite telemetry, the Kalman filter is often used within a (linear) state-space modelling framework to refine location estimates and reconstruct

movements, under the assumption that process and measurement errors are Gaussian (Jonsen et al., 2020). Particle filters generalise this methodology, providing a robust modelling framework that is well-suited to movement modelling in receiver arrays.

The particle filter approximates the distribution of interest with a set of discrete samples termed 'particles' (Doucet & Johansen, 2009). In an animal-tracking context, the filter approximates the (partial) marginal distribution of the individual's location ( $\mathbf{s}$ ) at time  $t$ , given all data ( $\mathbf{y}$ ) up to that time [i.e.  $f(\mathbf{s}_t | \mathbf{y}_{1:t})$ ]. The process model simulates particle movement over the landscape as a discrete-time Markovian walk [i.e.  $\mathbf{s}_t \sim f(\mathbf{s}_t | \mathbf{s}_{t-1})$ ] and the observation model, together with a resampling step, eliminates or duplicates particles in line with the likelihood [i.e.  $f(\mathbf{y}_t | \mathbf{s}_t)$ ]. By including multiple observation models, disparate datasets can be integrated to refine inferences. Subsequent smoothing algorithms approximate the full marginal distribution of the individual's location at time  $t$ , given all data from the start ( $t = 1$ ) to the end ( $t = T$ ) of the time series [i.e.  $f(\mathbf{s}_t | \mathbf{y}_{1:T})$ ]. Approximating the joint distribution [i.e. sampling individual trajectories from  $f(\mathbf{s}_{1:T} | \mathbf{y}_{1:T})$ ] is also possible, but computationally more expensive.

Particle filters have received limited attention in ecology (Andersen et al., 2007; Liu et al., 2019). In the field of acoustic telemetry, only one study explored the approach (Lavender et al., 2023). That study proposed a two-branch framework for reconstructing movements, comprising an acoustic-container (AC) branch algorithm that resolved the possible locations for an individual, given the data, and a particle filter (PF) branch algorithm that incorporated movement. Different combinations of AC-branch and PF-branch algorithms were collectively termed the 'flapper algorithms' and include the ACPF algorithm (which incorporates acoustic data) and the acoustic-container depth-contour (ACDC) PF algorithm (which incorporates acoustic and archival data). Here, we simply use the abbreviations AC and ACDC as generic labels for inference (particle) algorithms that incorporate acoustic or both acoustic and archival data (with or without smoothing).

This study develops the use of particle algorithms for movement modelling in passive acoustic telemetry systems. Our methodology formalises and extends the 'flapper algorithms' within a particle filtering-smoothing framework that (i) accounts for movement within and between periods of detection, (ii) models the detection process and (iii) facilitates the integration of disparate datasets. In a simulation analysis, we validate the approach, analyse method performance and explore algorithm behaviour. The results confirm particle algorithms outperform alternatives and represent a new state-of-the-art for movement modelling in passive acoustic telemetry systems.

## 2 | MATERIALS AND METHODS

### 2.1 | Overview

We formulate a Bayesian state-space model for the state (location) of a tagged animal in an acoustic telemetry system. Individual locations are denoted by  $\mathbf{s}$ . We consider the two-dimensional vector

$\mathbf{s} = (s_x, s_y)$ , where  $s_x$  and  $s_y$  are continuous. The movement process is represented as a regular series of steps from time  $t = 1$  to  $t = T$ , each of duration  $\Delta t$ , by  $f(\mathbf{s}_{1:T})$ , where  $f$  is a probability density function. Contingent upon the individual's location, observations ( $\mathbf{y}$ ), such as detections, are recorded at regular or irregular intervals. The objective is to infer the locations of the animal, using our knowledge of the movement process and the observations. Here, we formalise a model for this objective and a sampling algorithm. In Sections 1–5 in Data S1, we provide algorithmic details for mathematical and non-mathematical readers. For a notational summary, see Table S1.

## 2.2 | Model

### 2.2.1 | Objective

Our objective is to derive the joint probability distribution  $f(\mathbf{s}_{1:T} | \mathbf{y}_{1:T})$  of a tagged individual's possible trajectories from the start to the end of the time series, accounting for the movement process and the observations. Using Bayes' theorem, the joint distribution can be expressed in terms of a prior (the movement process) and a likelihood (the observation process):

$$f(\mathbf{s}_{1:T} | \mathbf{y}_{1:T}) \propto f(\mathbf{s}_{1:T}) f(\mathbf{y}_{1:T} | \mathbf{s}_{1:T}). \quad (1)$$

### 2.2.2 | Movement process

The expression  $f(\mathbf{s}_{1:T})$  represents movement. We model  $f(\mathbf{s}_{1:T})$  as a discrete-time Markovian process

$$f(\mathbf{s}_{1:T}) = f(\mathbf{s}_{t=1}) \prod_{t=2}^T f(\mathbf{s}_t | \mathbf{s}_{t-1}), \quad (2)$$

where  $f(\mathbf{s}_{t=1})$  is a probability density function of the individual's starting location and  $f(\mathbf{s}_t | \mathbf{s}_{t-1})$  is the probability density of moving from  $\mathbf{s}_{t-1} \rightarrow \mathbf{s}_t$ . A simple model for  $f(\mathbf{s}_t | \mathbf{s}_{t-1})$  is a restricted two-dimensional random walk, in which the location  $\mathbf{s}_t$  is given by

$$\mathbf{s}_t = (s_{x,t-1} + d_t \cos \phi_t, s_{y,t-1} + d_t \sin \phi_t), \quad (3)$$

where  $d$  and  $\phi$  are independently distributed random variables that represent step lengths and headings, subject to boundary conditions (i.e. land). Here, we use a Gamma step-length distribution based on pre-defined shape ( $k$ ) and scale ( $\theta$ ) parameters and a truncation interval defined between zero and mobility:

$$d_t \sim \text{Truncated Gamma}(k, \theta, 0, \text{mobility}), \quad (4)$$

where mobility is the maximum distance the individual can move in one time step. For the heading, we use a uniform distribution:

$$\phi_t \sim \text{Uniform}(-\pi, \pi). \quad (5)$$

We assume that the prior can be parameterised by combining available datasets (from field observations, fine-scale positioning,

video footage, accelerometry, laboratory studies and other sources), literature and expert knowledge of studied species and related taxa.

### 2.2.3 | Observation process

#### Joint likelihood

The term  $f(\mathbf{y}_{1:T} | \mathbf{s}_{1:T})$  denotes the joint likelihood. This measures the probability of the observations given the locations of the individual ( $\mathbf{s}_{1:T}$ ). We assume the observations, conditional on  $\mathbf{s}_{1:T}$ , are independent and express  $f(\mathbf{y}_{1:T} | \mathbf{s}_{1:T})$  as the product of the likelihood from each time step:

$$f(\mathbf{y}_{1:T} | \mathbf{s}_{1:T}) = \prod_{t=1}^T f(\mathbf{y}_t | \mathbf{s}_t). \quad (6)$$

Observations may include acoustic records and ancillary data, such as depth measurements. Acoustic observations comprise detections, which are explicitly recorded, and non-detections, which are implicitly known for each  $t$  (assuming  $\Delta t$  exceeds the transmission interval). We use  $\mathbf{y}^{(A)}$  to denote an  $M \times T$  matrix of acoustic observations, where  $M$  is the number of receivers, and  $\mathbf{y}^{(D)}$  to denote a row vector of depth observations (from 1, ...,  $T$ ). Both sets of observations form the dataset  $\mathbf{y} = \{\mathbf{y}^{(A)}, \mathbf{y}^{(D)}\}$ . The combined likelihood at time  $t$  is given by

$$f(\mathbf{y}_t | \mathbf{s}_t) = f(\mathbf{y}_t^{(A)} | \mathbf{s}_t) f(\mathbf{y}_t^{(D)} | \mathbf{s}_t), \quad (7)$$

where  $\mathbf{y}_t^{(A)}$  is a column vector of acoustic observations at time  $t$  and  $\mathbf{y}_t^{(D)}$  is the depth observation.

#### Acoustic observations

The acoustic likelihood expresses the correspondence between acoustic observations and latent locations. We denote a detection at receiver  $k$  as  $y_{k,t}^{(A)} = 1$  and non-detection as  $y_{k,t}^{(A)} = 0$ . We assume detections are Bernoulli distributed and express the probability of the observation  $y_{k,t}^{(A)} \in \{0, 1\}$  at receiver  $k$  as:

$$f(y_{k,t}^{(A)} | \mathbf{s}_t) = p_{k,t}(\mathbf{s}_t)^{y_{k,t}^{(A)}} (1 - p_{k,t}(\mathbf{s}_t))^{1 - y_{k,t}^{(A)}}. \quad (8)$$

Detection probability ( $p$ ) is modelled as a function of covariates. A simple model for  $p$  is a logistic function of the distance between the receiver's location ( $\mathbf{r}_k = (s_{x,k}, s_{y,k})$ ) and transmitter ( $\mathbf{s}$ ), that is

$$p_{k,t}(\mathbf{s}_t) = \begin{cases} \left(1 + e^{-(\alpha - \beta \times h(\mathbf{s}_t, \mathbf{r}_k))}\right)^{-1} & \text{if } h(\mathbf{s}_t, \mathbf{r}_k) < \gamma \\ 0 & \text{otherwise} \end{cases}, \quad (9)$$

where  $h(\cdot, \cdot)$  is a distance function;  $\alpha$  and  $\beta$  are parameters; and  $\gamma$  is the detection range (Lavender et al., 2023). We assume these parameters can be set from range tests, expert knowledge and literature (Kessel

et al., 2014). Where data are available, spatiotemporal variation in detection probability is easy to model with detection parameters that vary over space ( $\mathbf{s}_t, \mathbf{r}_k$ ) or time ( $t$ ).

The combined probability of all acoustic observations is the product of independent probabilities from each receiver:

$$f(\mathbf{y}_t^{(A)} | \mathbf{s}_t) = \prod_k f(y_{k,t}^{(A)} | \mathbf{s}_t), \quad (10)$$

where  $k$  indexes over operational receivers at time  $t$ .

### Depth observations

The depth likelihood expresses the correspondence between each depth observation  $y_t^{(D)}$  and the latent location. An example model for the probability density of  $y_t^{(D)}$  is

$$f(y_t^{(D)} | \mathbf{s}_t) = \begin{cases} z_t & \text{if } b(\mathbf{s}_t) - \epsilon_{\text{shallow}}(\mathbf{s}_t) \leq y_t^{(D)} \leq b(\mathbf{s}_t) + \epsilon_{\text{deep}}(\mathbf{s}_t) \\ 0 & \text{otherwise} \end{cases}, \quad (11)$$

where  $z_t = (\epsilon_{\text{deep}}(\mathbf{s}_t) + \epsilon_{\text{shallow}}(\mathbf{s}_t))^{-1}$ . This model requires  $y_t^{(D)}$  to be within an envelope around the bathymetric depth  $b(\mathbf{s}_t)$  defined by the shallow and deep depth-adjustment functions,  $\epsilon_{\text{shallow}}(\mathbf{s}_t)$ ,  $\epsilon_{\text{deep}}(\mathbf{s}_t) \leq b(\mathbf{s}_t)$ . These functions capture observational uncertainty and spatially explicit bathymetric uncertainty and can be tailored to species with different lifestyles: for benthic species, observations must be close to the seabed, which can be enforced by small errors ( $\epsilon_{\text{shallow}}(\mathbf{s}_t), \epsilon_{\text{deep}}(\mathbf{s}_t) \ll b(\mathbf{s}_t)$ ); for pelagic species, observations may occur in the water column, which is permitted by larger  $\epsilon_{\text{shallow}}(\mathbf{s}_t)$  values. As for the acoustic observation model, ancillary observation models should be parameterised from available datasets, expert knowledge and literature.

## 2.3 | Sampling algorithm

### 2.3.1 | Filtering

We have formulated a model for the joint distribution of the individual's locations, given all data [i.e.  $f(\mathbf{s}_{1:T} | \mathbf{y}_{1:T})$ ]. We now outline a sampling algorithm. The target of our inference is location; we assume static parameters are known. For inference, we begin with the simpler, partial marginal distribution  $f(\mathbf{s}_t | \mathbf{y}_{1:t})$ . This is recursively represented as

$$f(\mathbf{s}_t | \mathbf{y}_{1:t}) \propto \left( \int f(\mathbf{s}_{t-1} | \mathbf{y}_{1:t-1}) f(\mathbf{s}_t | \mathbf{s}_{t-1}) d\mathbf{s}_{t-1} \right) f(\mathbf{y}_t | \mathbf{s}_t). \quad (12)$$

The particle filter approximates  $f(\mathbf{s}_t | \mathbf{y}_{1:t})$  as a sum of  $N$  weighted samples, termed 'particles', that is,

$$f(\mathbf{s}_t | \mathbf{y}_{1:t}) \approx \sum_i^N \delta(\mathbf{s}_t - \mathbf{s}_{i,t}) w_i, \quad (13)$$

where  $\delta$  is the Dirac delta function,  $w$  denotes normalised weights ( $\sum_i w_i = 1$ ) and  $i$  indexes particles, which represent possible locations for

the individual. This is a recursive procedure (derived from Equation 12) that at each time step comprises three stages:

- *Simulation (movement)*. We simulate particles, following Equations (2–5). Initial particles are sampled from a probability distribution, such as a uniform distribution, via  $\mathbf{s}_{i,t=1} \sim f(\mathbf{s}_{t=1})$ . At subsequent time steps, we simulate particles from the movement process, that is  $\mathbf{s}_{i,t} \sim f(\mathbf{s}_{i,t} | \mathbf{s}_{i,t-1})$ , using a movement model, such as a random walk (Equation 3).
- *Weighting (observation)*. Particles are weighted in line with the likelihood, that is  $w_{i,t} \propto w_{i,t-1} f(\mathbf{y}_t | \mathbf{s}_{i,t})$ , following Equations (6–11).
- *Resampling*. Periodically, weighted particles are re-sampled. This procedure eliminates unlikely particles and duplicates likely ones.

The time complexity of the particle filter is  $\mathcal{O}(NT)$  (Doucet & Johansen, 2009).

The end result is a set of particles (location samples) from  $f(\mathbf{s}_t | \mathbf{y}_{1:t})$  that represent an individual's possible locations at each time step, given all preceding and contemporary data. Theoretically, a small number of particles ( $N \approx 1000$ ) is sufficient to approximate a two-dimensional distribution, of the kind described here, but in practice many more particles may be required to ensure that sufficient particles remain 'alive' at each time step to approximate  $f(\mathbf{s}_t | \mathbf{y}_{1:t})$ ; that is, to achieve convergence.

### 2.3.2 | Smoothing

Particle smoothing re-weights particles from the filter to approximate the full marginal,  $f(\mathbf{s}_t | \mathbf{y}_{1:T})$  (Doucet & Johansen, 2009). The two-filter smoother uses  $N$  particles ( $\mathbf{s}_{i,t}$ ) from a forward filter run (with weights  $w_{i,t}$ ) and  $N$  particles ( $\tilde{\mathbf{s}}_{j,t}$ ) from a backward run (with weights  $\tilde{w}_{j,t}$ ) to obtain a set of smoothing weights ( $\tilde{w}_{j,t|T}$ ):

$$\tilde{w}_{j,t|T} \approx \tilde{w}_{j,t} \sum_i^N f(\tilde{\mathbf{s}}_{j,t} | \mathbf{s}_{i,t-1}) w_{i,t-1}. \quad (14)$$

For each particle  $\tilde{\mathbf{s}}_{j,t}$ , these weights effectively sum over all possible movements from the preceding particles on the forward filter. The distribution  $f(\mathbf{s}_t | \mathbf{y}_{1:T})$  is approximated as a weighted sum of smoothed particles:

$$f(\mathbf{s}_t | \mathbf{y}_{1:T}) \approx \sum_j^N \delta(\mathbf{s}_t - \tilde{\mathbf{s}}_{j,t}) \tilde{w}_{j,t|T}. \quad (15)$$

The time complexity of smoothing is  $\mathcal{O}(N^2T)$  (Doucet & Johansen, 2009). However, typically only a subset of the particles required for a successful run of the filter is required for an effective approximation of  $f(\mathbf{s}_t | \mathbf{y}_{1:T})$ .

## 2.4 | Mapping

Particles can be used to reconstruct movements and map space use. For mapping, we suggest the 'probability-of-use' metric ( $P$ ), which

represents the probability that an individual is located in a given location at a randomly chosen time. This can be calculated across a grid as a weighted average of the particles in each cell:

$$P_l = \frac{1}{T} \sum_{i,t} \delta_{l,i,t} w_{i,t}^* \quad (16)$$

where  $l$  indexes grid cells,  $l_{i,t}$  is the grid cell of particle  $i$  at time  $t$ ,  $\delta_{l,i,t}$  is the Kronecker delta and  $w_{i,t}^*$  is the weight of that particle at time  $t$  (either  $w_{i,t}$ ,  $\tilde{w}_{j,t}$  or  $\tilde{w}_{j,t|T}$ ). Particles may be derived from the filter [approximating  $f(\mathbf{s}_t | \mathbf{y}_{1:t})$ ] or the smoother [approximating  $f(\mathbf{s}_t | \mathbf{y}_{1:T})$ ], which is more expensive but produces refined maps of space use. In practice,  $P_l$  is sensitive to grid resolution and we suggest computing  $P_l$  across a fine grid followed by kernel smoothing (see Section 6 in Data S1).

## 2.5 | Simulations

### 2.5.1 | Software

We developed the patten R package and the Patter.jl backend to implement the methodology (Lavender et al., 2024a). Here we illustrate and evaluate algorithm performance and sensitivity by simulation, using R, v.4.3.1 (R Core Team, 2023). Code is available online (Lavender et al., 2024b).

### 2.5.2 | Study systems

In all simulations, we considered a 100 km<sup>2</sup> rectangular area and a 10 × 10 m bathymetric grid. Within this area, we considered two hypothetical 'study systems' defined by distinct movement and observational processes, for a hypothetical benthic animal and acoustic and archival data (Figure S1; Table S2). (Two study systems were considered to validate the robustness of our simulations to the parameters characterising any one system.) Both movement processes were defined by a discrete-time, continuous-space Markovian random-walk model (Equations 2–5), with the individual taking a 'step' up to 'mobility' metres in length every 2 min, over a 2-day period (Table S2). The detection process was binomial, with detection probability declining logistically to zero by  $\gamma$  metres from receiver(s), following Equation (9) (Table S2). The archival observation process was uniform and constant across all simulations (Table S2). In each system, we simulated 20 acoustic arrays with 10, 20, ..., 100 receivers, arranged randomly or regularly (Figure S2; Table S3). In each system and for each array, we simulated 30 realisations of the movement process (30 movement paths) and 30 corresponding realisations of the observation processes (30 acoustic and archival datasets). We only considered the simulated paths and observations between the first and last detection and simulations which generated >10 detections.

### 2.5.3 | Performance

We compared patterns of space use exhibited by simulated paths to those reconstructed from simulated observations by two heuristic algorithms (COAs and RSPs) and our AC and ACDC particle algorithms (including filtering and filtering–smoothing implementations). For simulated paths, 'true' patterns of space use were generated by fitting kernel UDs to path coordinates using cross-validation. These UDs were compared against the UDs generated from each algorithm, visually and with standard error metrics: mean bias, mean error, root mean square error, Spearman's rank correlation coefficient and the index of agreement. The main text focuses on mean error (ME), which distinguished algorithms most effectively. However, all metrics told similar stories. For details, see Sections 7 and 8 (Data S1) and Table S4.

### 2.5.4 | Sensitivity

For a subset of arrays, we analysed particle algorithm sensitivity. The purpose of this analysis was to investigate how patterns of space use change if static parameters in the movement and observation models (such as  $\gamma$ ), which are assumed known, are overly restrictive or flexible. To investigate algorithm sensitivity, we compared UDs for simulated paths to those reconstructed by particle filtering–smoothing algorithms with mis-specified movement ( $k, \theta, \text{mobility}$ ) and acoustic observation ( $\alpha, \beta$  and  $\gamma$ ) parameters, qualitatively and with ME (Figure S3; Table S5). This analysis reveals the extent to which patterns of space use are sensitive to selected parameters and which parameters should therefore be prioritised in data-collection efforts.

## 3 | RESULTS

### 3.1 | Performance

In the visual analysis of UDs, heuristic methods were consistently outperformed by particle algorithms (Figure 1; Figure S4). In the sparse arrays (with 10 receivers: Figure 1a–l), COAs concentrated in specific areas and poorly represented underlying patterns, irrespective of receiver arrangement (e.g. Figure 1a vs. Figure 1b). RSP maps also misplaced hotspots, concentrating them around receivers, but by smoothing the connections between receivers, they better represented those transitions and exhibited lower ME (e.g. Figure 1c). Particle algorithms suggested more nuanced patterns (e.g. Figure 1d,e). Maps based on particles from the filter [approximating  $f(\mathbf{s}_t | \mathbf{y}_{1:t})$ ] were relatively diffuse, but more accurately placed hotspots away from receivers, resulting in an ME similar to RSPs (Figure S4). Smoothed particles [approximating  $f(\mathbf{s}_t | \mathbf{y}_{1:T})$ ] produced more refined maps, with lower ME than RSPs in both random and regular arrays (Figure 1d–f,j–l). Compared to the AC algorithm, the ACDC algorithm suggested more precise patterns of space use (Figure 1e,k; Figures S2 and S4).

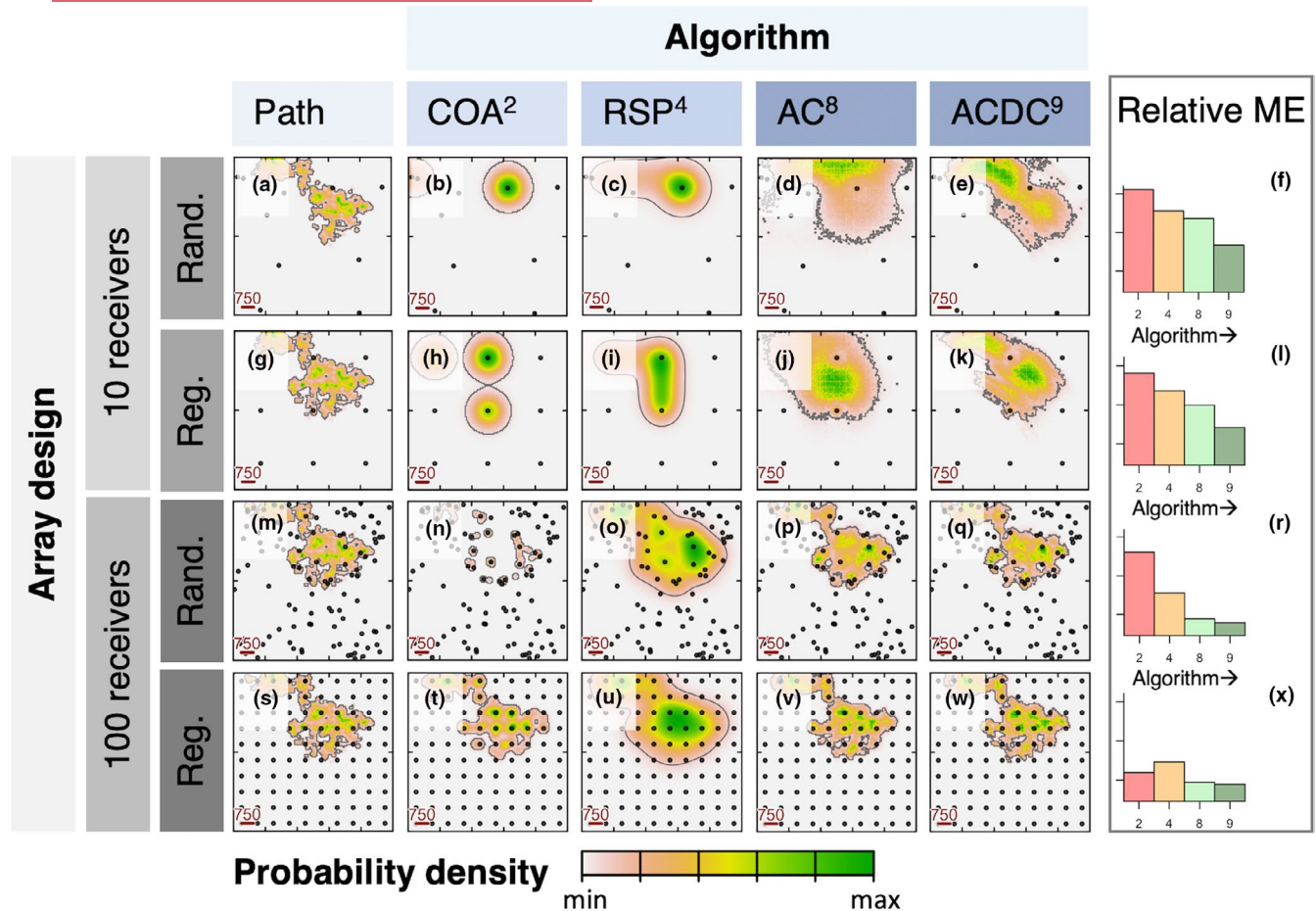


**FIGURE 1** Utilisation distributions (UDs) reconstructed by different algorithms in selected array designs for a hypothetical study system. Four designs with 10 or 100 receivers in random or regular arrangements are shown. For each array (row), the estimated UD for the portion of the simulated path between the first and last detections is shown, alongside comparable UD generated by the COA, RSP and particle filtering–smoothing algorithms (AC and ACDC). Lines mark home ranges (and contain 95% of the probability density volume). Points mark receivers. The detection range was 750 m. Bar plots show relative mean error (ME). Algorithm superscripts identify selected algorithm implementations (of which there were nine in total), following Table S4. Panels correspond to the first simulated study system. For the full figure, see Figure S4.

In the dense arrays (with 100 receivers), all algorithms represented underlying patterns more effectively (Figure 1m–x; Figure S4). For the COA algorithm, there was a clear influence of receiver arrangement, with heavy fragmentation (and high ME) in the random array (Figure 1n) and smoother patterns (and lower ME) in the regular array (Figure 1t). RSPs behaved similarly in the two array designs, broadly capturing but over-smoothing simulated movements (Figure 1o,u). Accordingly, the COA maps were worse than RSP maps in the random array (Figure 1r) but marginally better in the regular array according to ME (Figure 1x). Particle algorithms performed more effectively in both array designs, producing accurate maps that closely correspond to those for the simulated path (Figure 1p–r,v–x). Differences between maps from the filter and smoother were limited (Figure S4).

In illustrated arrays (with 10 or 100 receivers), a consistent ranking of algorithms emerged from repeated simulations of the same data-generating processes (Figure 2; Figure S5). In the

sparse arrays (with 10 receivers), the COA algorithm generally produced the highest ME (occasionally even exceeding a null model) (Figure 2a,b). RSPs and particle algorithms produced overlapping but lower MEs (Figure 2a,b). In general, the particle filter produced similar (AC) or lower (ACDC) MEs compared to RSPs. Smoothing for both AC and ACDC algorithms resulted in lower MEs. In the dense arrays (with 100 receivers), ME was consistently lower (Figure 2c,d). In the dense, random array, the COA algorithm produced the highest MEs (Figure 2c). RSPs performed better but were outperformed by all particle algorithm implementations (Figure 2c). In the dense, regular array, COAs performed more effectively and marginally better than RSPs, but both were outperformed by the particle algorithms (Figure 2d). In both random and regular dense array designs, particle smoothing lowered ME. Maps from the ACDC algorithm exhibited lower ME than those from the AC algorithm, but this effect was limited. This result is expected in regions with a smooth bathymetry (as simulated here),

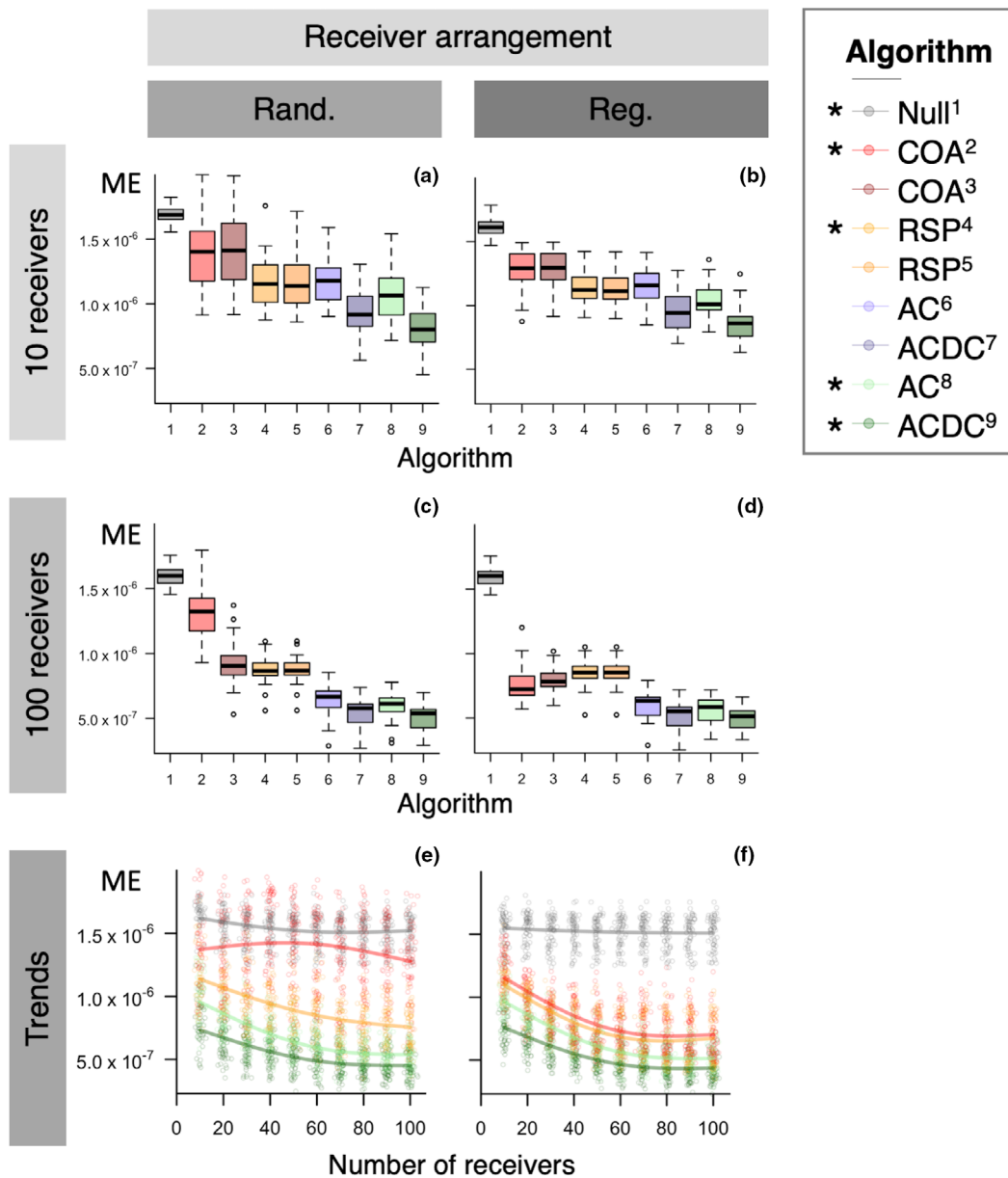


**FIGURE 2** The distribution of mean error (ME) across simulated arrays. Panels (a–d) show the distribution of ME across 30 realisations of the same data generating processes in four example arrays, with 10 or 100 receivers in random or regular arrangements, for nine algorithms. ME was calculated from comparison of each simulated path's UD (within the duration defined by the first and last detection) and the corresponding UD reconstructed by an algorithm. Boxplot width is proportional to the number of successful algorithm implementations. Algorithm numbers follow Table S4. Panels (e, f) show the trend in ME across array designs with different numbers of receivers for a subset (\*) of algorithms. Points mark ME values for specific comparisons and smoothers show the trend in expected ME. All panels correspond to the first simulated study system. For full details, see Figures S5 and S6.

which effectively spreads out the locational information provided by depth observations. These patterns were borne out by alternative error metrics (Figure S5) and across all simulated arrays (Figure 2e,f; Figure S6).

Out of 1181 performance simulations, only one AC and one ACDC simulation failed to converge with the selected number of particles on the first implementation. Run time (per time step) for the filter averaged 0.011s for AC (5000 particles) and 0.045s for ACDC (30,000 particles). Wall time for smoothing (1000 particles) averaged 0.237s per time step (Figure S7).

### 3.2 | Sensitivity

In the sensitivity analysis, severe parameter mis-specification caused convergence failures (Figure S8). In the movement process, convergence was most sensitive to under-estimation of mobility, followed by  $\theta$  and  $k$  and was insensitive to array design. In the acoustic observation model, convergence failures were associated with overly steep (deflated  $\alpha$ , inflated  $\beta$ ), overly shallow (inflated  $\alpha$ , deflated  $\beta$ ) and overly truncated (deflated  $\gamma$ ) detection probability functions, but the latter two types of mis-specification were most

problematic. Overly shallow functions are principally problematic because they excessively restrict particle samples from within detection containers in the gaps between detections (when the influence of  $\gamma$  is minimal). In contrast, overly truncated functions are principally problematic at the moment of detection because the  $\gamma$  parameter imposes a hard restriction on the region within which particles are sampled (unlike a deflated  $\alpha$  or inflated  $\beta$  value). These effects were generally more common in arrays with more receivers. For both movement and observation parameters, convergence failures were more common for ACDC (rather than AC) algorithm implementations, with the additional incorporation of depth observations effectively enhancing the chances of prior-data conflicts when the former is mis-specified.

Within the parameter space compatible with the data, parameter mis-specification affected patterns of space use (Figures S9–S14). In the movement process, parameter under-estimation produced more concentrated patterns (Figures S9–S11). In the observation process, steeper detection probability functions (deflated  $\alpha$ , inflated  $\beta$ ) concentrated hotspots around receivers while shallower functions (inflated  $\alpha$ , deflated  $\beta$ ) produced depressions in these areas (Figures S12 and S13). (This reflects the way that overly shallow functions restrict particle sampling within detection containers in the gaps between detections, which typically span the majority of a time series.) These effects were more noticeable in regular arrays. Under-estimation of  $\gamma$  concentrated patterns around receivers, but over-estimation had a limited effect (Figure S14). This result fits with the weakly truncating effect of  $\gamma$  in our simulations. In all simulations, ACDC-derived maps of space use were more robust to parameter mis-specification than AC-derived maps (Figures S9–S14).

Across the simulations, we observed a U-shaped relationship between ME and the degree of parameter mis-specification, relative to the true value (Figures S15 and S16). For movement parameters, ME grew more quickly with parameter under-estimation, especially in arrays with more receivers (Figure S15). Parameter over-estimation, which spreads out the low-probability edges of distributions, produced smaller increases in ME. In the acoustic observation process, ME grew most quickly as detection functions were made shallower (inflated  $\alpha$ , deflated  $\beta$ ) and was greatest in arrays with intermediate numbers of receivers (Figure S16). Under-estimation of  $\gamma$  also produced high MEs for the portion of algorithm runs that converged, while over-estimation had little influence.

In almost all cases, mis-specified particle algorithms continued to outperform heuristic methods in terms of ME (Figure S17).

## 4 | DISCUSSION

This study establishes a particle filtering–smoothing methodology for movement modelling in receiver arrays. The methodology represents the movement and detection processes in these systems within a probabilistically sound, flexible and intuitive framework. The process-based perspective marks a shift from the heuristic methods typically used for analysis in passive acoustic telemetry

systems (Kraft et al., 2023). The particle methodology reconstructs movements and patterns of space use within and between periods of detection. This produces more accurate maps of space use and facilitates analyses of home ranges, site affinity and habitat preferences. These developments should support research into the movement ecology and conservation of many species (Hays et al., 2019; Nathan et al., 2022).

The core conceptual advantage of our framework over heuristic approaches is the process-based perspective, which produces outputs with a clear statistical and biological interpretation (Hostetter & Royle, 2020; Lavender et al., 2023). The representation of movement is particularly important. Receiver arrays are often irregular and non-overlapping and ignoring movements or assuming direct transitions between receivers in these settings can suggest overly restrictive patterns of space use that are unduly influenced by array design and for which it is difficult to quantify uncertainty (Lavender et al., 2023). Modelling movements also facilitates analyses of residency—not only around receivers, as quantified by existing indices—but in wider regions of interest (Lavender et al., 2023). This is particularly important where arrays are deployed to inform conservation measures, such as Marine Protected Areas (Lavender et al., 2021a; Lea et al., 2016). Representation of the observation processes is also important. In the acoustic telemetry literature, imperfect detectability is acknowledged and quantified using range tests (Kessel et al., 2014), but it is typically ignored in analyses, which can bias inferences (Winton et al., 2018). Ancillary datasets are also almost exclusively ignored, despite their potential to refine position estimates (Aspillaga et al., 2019; Lavender et al., 2023).

For modelling patterns of space use, our results provide a substantive assessment of the performance of common heuristic methods and demonstrate the benefits of our statistical methodology. We show that the COA algorithm performs poorly relative to alternatives across the board. In sparse, irregular arrays, this algorithm is sometimes worse than a null model and barely improves with receiver number. The widespread adoption of this method and its promotion as the centre of a universally applicable analytical framework for passive acoustic telemetry therefore appear misplaced (Udyawer et al., 2018). Particularly in irregular arrays, even a simple representation of movement, as in RSPs, improves maps of space use. In arrays with more receivers, movement-orientated methods also improve more quickly than the COA algorithm and continue to represent underlying patterns of space use more faithfully. These results indicate that, in most real-world settings, the movement process contains valuable information and should be represented in analyses. Both COA and RSP algorithms were outperformed by particle algorithms, especially in irregular arrays. This performance difference was increased by the inclusion of the depth observations, even in the smooth bathymetric landscape we simulated. Given continued improvements in technology and the increasing wealth of data collected alongside acoustic detections (Matley et al., 2023), this is an encouraging result. The integration of state-space models for acoustic detections with ancillary data holds considerable future promise.

This is not to say that heuristic methods should be superseded by state-space models. Heuristic methods have a track record in the literature (Kraft et al., 2023; Udyawer et al., 2018) and conservation science (Lavender et al., 2021a; Lea et al., 2016). They are quick to apply and may indicate similar patterns of space use to state-space models when data are particularly sparse (and all approaches struggle) or dense (and the prior's contribution is dampened). Performance can also be improved by tuning parameters on a case-by-case basis. For these reasons, we maintain that different methods are more or less useful in different contexts and caution that analytical standardisation, while often valuable, is not always appropriate. Building on this study, we call for further research into the utility of alternative methods in different settings.

This study unifies and enhances the 'flapper' algorithms within a formal particle filtering-smoothing methodology (Lavender et al., 2023). This methodology integrates the 'AC branch' and 'PF-branch' algorithms within a single, mathematically coherent framework (Lavender et al., 2023). On a practical level, this reformulation improves algorithm efficiency and facilitates the integration of disparate datasets. In the flapper algorithms, AC-branch algorithms were required to define the possible locations of an individual, given the data, across a grid at each time step, which becomes prohibitively expensive with increasing grid size. In the particle filter, particle simulation and the likelihood evaluations achieve the same objective but are restricted to particle locations, which removes the dependence on grid size. By recasting the flapper algorithms in their entirety as a particle methodology, we can also start to exploit advanced developments in this field. The refinement of patterns of space use by coupling filtering and smoothing demonstrates the potential in this area. This innovation also links movement modelling in acoustic telemetry systems to the handful of particle algorithms developed for animal tracking in other systems and suggests potential refinements (such as two-filter smoothing) that may support applications in those systems (Andersen et al., 2007; Liu et al., 2019).

Our methodology is related to existing state-space modelling studies in the acoustic telemetry literature (Alós et al., 2016; Hostetter & Royle, 2020; Pedersen & Weng, 2013). The main differences are the formulation of the sub-models (which is system-specific), the incorporation of ancillary data and the inference method. For example, Alós et al. (2016) and Hostetter and Royle (2020) fit state-space models to acoustic observations using Just Another Gibbs Sampler (JAGS). In theory, this approach benefits from data-driven parameter estimation and directly samples the joint distribution,  $f(\mathbf{s}_{1:T} | \mathbf{y}_{1:T})$ . However, JAGS often explores correlated distributions inefficiently and can be prohibitively expensive in real-world settings. In contrast, the particle filtering-smoothing methodology targets the simpler distribution  $f(\mathbf{s}_t | \mathbf{y}_{1:T})$  but can be orders of magnitude faster (Lavender et al., 2024a).

There are practical challenges to the use of particle filters. The main biological challenge is the formulation of the movement and observation sub-models. In a state-space modelling framework, these models must be explicitly defined—unlike heuristic methods, where movement capacities and observational processes are enveloped by

'tuning parameters' or considered at the interpretation stage (Niella et al., 2020; Simpfendorfer et al., 2002). Model parameterisation is a related challenge. While it is possible to infer model parameters and locations jointly via Bayesian inference or maximum likelihood, in a particle filtering context, this is computationally expensive. In sparse receiver arrays, the information available to parameterise these models is also limited. The present formulation of our filter, therefore, requires parameters to be specified a priori from available datasets, expert knowledge and/or literature. For example, in a study of movement patterns in a Critically Endangered skate (*Dipturus intermedius*), we integrated information from previous studies and literature to parameterise our models (Lavender et al., 2021a, 2021b, 2025). The movement model was informed by analyses of movement rates between receivers and vertical activity, plus hydrodynamic modelling of flow velocity and information in the literature for related species (from accelerometry, satellite tracking, flow tank experiments and trawl footage). In the absence of direct measurements, these studies helped to bound our expectations for movement rates. For other species, such as lake trout (*Salvelinus namaycush*), fine-scale positioning studies, accelerometer measurements and swim-tunnel calibrations are available (Blanchfield et al., 2023). Observation models also require parameterisation a priori. Acoustic observation models benefit from in-situ range tests, plus a wide literature on detection probability informed by theoretical considerations and manufacturer guidelines (Kessel et al., 2014). Accordingly, in our skate research, we drew on these information sources to set the detection probability model (Lavender et al., 2025). Observation models for ancillary datasets should be parameterised similarly.

Our simulations provide reassurance and guidance to practitioners formulating system-specific sub-models when parameters are uncertain. For the movement process, we found that the overly flexible movement model outperformed the overly restrictive one (in terms of ME), suggesting that some flexibility in the movement model may be preferable when parameters are uncertain. For the acoustic observation model, in our simulations (with sparse detections), we found the shape of the detection probability function was more important than the detection range, providing the detection range was large enough. Where data are lacking, we therefore recommend focusing data collection efforts on characterising the shape of the function and setting the detection range based on manufacturer specifications and the literature. That being said, the simulations show that even simplified or imperfect representations of the processes that generate observations can substantially refine maps of space use, while sensitivity analyses help quantify epistemic uncertainty. As more data are collected, model inferences can be further refined.

Particle degeneracy is a second challenge for particle filtering-smoothing algorithms (Doucet & Johansen, 2009). Degeneracy occurs when a minority of particles acquire the majority of the weight due to the compounding effects of mismatches between the movement and observational models. In the filter, particle degeneracy can make convergence hard to achieve with modest (<1 million) numbers of particles. During smoothing, particle degeneracy can similarly

lead to a situation where initial samples are dominated by a few particles. Common measures we have implemented to mitigate degeneracy include increasing particle number, low-variance adaptive resampling and two-filter smoothing (Doucet & Johansen, 2009).

Nevertheless, particle degeneracy can remain problematic. In this study, almost all simulations successfully converged, but elsewhere we have experienced challenges coupling sparse acoustic observations with relatively informative archival datasets for benthic species (Lavender et al., 2025). During detection gaps, such situations permit a labyrinth of possible routes that particles have to explore but ultimately render few of them compatible with the data. In these situations, Hamiltonian Monte Carlo (HMC) may be a preferable implementation algorithm (Betancourt, 2017). Like Gibbs sampling, HMC can be used to sample the high-dimensional space of trajectories but uses derivatives to make proposals, which is more efficient. HMC can also be used to sample model parameters simultaneously (Albert et al., 2015). State-space models for acoustic telemetry have yet to exploit HMC and this is a promising avenue for further research. However, theoretical and practical hurdles remain, including the specification of starting values, the requirement for smooth likelihood functions, multimodality and the curse of dimensionality. At the current time, estimation of latent locations in complex environments with relatively informative ancillary datasets therefore remains a hard problem for Bayesian sampling methods and alternative approaches may be required (Pedersen et al., 2008). However, in many other situations, including the analyses in this study, these considerations are less relevant because particles can move around available routes more freely (when ancillary data are less informative) or are restricted to fewer possibilities (when ancillary data are highly informative).

A third challenge is that Bayesian techniques can be computationally expensive. The time complexity of the particle filter scales linearly with the number of particles [ $\mathcal{O}(NT)$ ] but most smoothing algorithms are more expensive [ $\mathcal{O}(N^2T)$ ] (Doucet & Johansen, 2009). In dense receiver arrays where particle trajectories are relatively constrained, our simulations suggest that particle filtering may be sufficient, but in other situations smoothing substantially improves maps of space use. In this study, we averaged 0.01–0.05 s per time step on the particle filter (with 5000–30,000 particles) and 0.24 s for smoothing (with 1000 particles) in single-threaded mode on a standard personal computer. While further computational optimisation remains desirable, these speeds compare favourably with related routines for fitting state-space models (Hostetter & Royle, 2020; Liu et al., 2019) and make particle algorithms serious candidates for substantive, real-world analyses (Lavender et al., 2024a).

Looking ahead, we anticipate significant opportunities for continued theoretical and applied work in this area. There is scope to tailor the movement model for different applications through the incorporation of three-dimensional states for demersal and pelagic species (Aspillaga et al., 2019) and behaviour (Lavender et al., 2025). In the representation of the observational processes, one could account for random acoustic transmission intervals, if required (Hostetter & Royle, 2020) and incorporate diverse datasets, such as

temperature or salinity (Lavender et al., 2023). The development of multi-resolution models that resolve movements at high resolution in acoustic arrays and use sparse ancillary observations to model larger-scale movements is another important area for future work (Pedersen et al., 2008). Joint inference of movement, observation, and state parameters may also be desirable in situations where prior knowledge is limited and data are sufficient. Our particle algorithms stand to benefit from a growing literature, which includes gradient-based methods and other techniques with enhanced convergence properties, as well as novel smoothing approaches (Maken et al., 2022). More broadly, significant work remains to investigate how we can improve, optimise and apply the suite of existing methods in different study systems. We point readers interested in applying our methods to the accompanying software packages (Lavender et al., 2024a).

#### AUTHOR CONTRIBUTIONS

Edward Lavender conceived the study and developed the methodology with Andreas Scheidegger, Carlo Albert and Helen Moor (Principal Investigator). This was motivated by work on the Movement Ecology of Flapper Skate project established by James Thorburn and an earlier modelling study led principally by Edward Lavender, Stanisław W. Biber, Janine Illian and Sophie Smout (Principal Investigator). In the current study, Edward Lavender led the analysis and writing of the manuscript. All authors contributed to drafts and approved publication.

#### ACKNOWLEDGEMENTS

We thank Stuart Dennis for scientific computing support.

#### FUNDING INFORMATION

EL was supported by a postdoctoral researcher position at Eawag, funded by the Department of Systems Analysis, Integrated Assessment and Modelling.

#### CONFLICT OF INTEREST STATEMENT

The authors declare no conflicts of interest.

#### PEER REVIEW

The peer review history for this article is available at <https://www.webofscience.com/api/gateway/wos/peer-review/10.1111/2041-210X.70028>.

#### DATA AVAILABILITY STATEMENT

Code available via <https://doi.org/10.5281/zenodo.13767598> (Lavender et al., 2024a).

#### ORCID

Edward Lavender  <https://orcid.org/0000-0002-8040-7489>

Andreas Scheidegger  <https://orcid.org/0000-0003-2575-2172>

Carlo Albert  <https://orcid.org/0000-0001-9160-9601>

Stanisław W. Biber  <https://orcid.org/0000-0001-5157-2904>

Janine Illian  <https://orcid.org/0000-0002-6130-2796>

James Thorburn  <https://orcid.org/0000-0002-4392-1737>

Sophie Smout  <https://orcid.org/0000-0002-5125-9827>

Helen Moor  <https://orcid.org/0000-0002-1340-2039>

## REFERENCES

- Abrahms, B., Aikens, E. O., Armstrong, J. B., Deacy, W. W., Kauffman, M. J., & Merkle, J. A. (2021). Emerging perspectives on resource tracking and animal movement ecology. *Trends in Ecology & Evolution*, 36(4), 308–320. <https://doi.org/10.1016/j.tree.2020.10.018>
- Albert, C., Ulzega, S., & Stoop, R. (2015). Boosting Bayesian parameter inference of nonlinear stochastic differential equation models by Hamiltonian scale separation. *Physical Review E*, 93, 043313. <https://doi.org/10.1103/PhysRevE.93.043313>
- Alós, J., Palmer, M., Balle, S., & Arlinghaus, R. (2016). Bayesian state-space modelling of conventional acoustic tracking provides accurate descriptors of home range behavior in a small-bodied coastal fish species. *PLoS One*, 11(4), e0154089. <https://doi.org/10.1371/journal.pone.0154089>
- Andersen, K. H., Nielsen, A., Thygesen, U. H., Hinrichsen, H.-H., & Neuenfeldt, S. (2007). Using the particle filter to geolocate Atlantic cod (*Gadus morhua*) in the Baltic Sea, with special emphasis on determining uncertainty. *Canadian Journal of Fisheries and Aquatic Sciences*, 64(4), 618–627. <https://doi.org/10.1139/f07-037>
- Aspillaga, E., Safi, K., Hereu, B., & Bartumeus, F. (2019). Modelling the three-dimensional space use of aquatic animals combining topography and Eulerian telemetry data. *Methods in Ecology and Evolution*, 10(9), 1551–1557. <https://doi.org/10.1111/2041-210X.13232>
- Betancourt, M. (2017). A conceptual introduction to Hamiltonian Monte Carlo. *arXiv*. <https://doi.org/10.48550/arXiv.1701.02434>
- Blanchfield, P. J., McKee, G., Guzzo, M. M., Chapelsky, A. J., & Cott, P. A. (2023). Seasonal variation in activity and nearshore habitat use of Lake trout in a subarctic lake. *Movement Ecology*, 11(1), 54. <https://doi.org/10.1186/s40462-023-00417-x>
- Doucet, A., & Johansen, A. (2009). A tutorial on particle filtering and smoothing: Fifteen years later. In D. Crisan & B. Rozovskii (Eds.), *The Oxford handbook of nonlinear filtering*. Oxford University Press.
- Hays, G. C., Bailey, H., Bograd, S. J., Bowen, W. D., Campagna, C., Carmichael, R. H., Casale, P., Chiaradia, A., Costa, D. P., Cuevas, E., Nico de Bruyn, P. J., Dias, M. P., Duarte, C. M., Dunn, D. C., Dutton, P. H., Esteban, N., Friedlaender, A., Goetz, K. T., Godley, B. J., ... Sequeira, A. M. M. (2019). Translating marine animal tracking data into conservation policy and management. *Trends in Ecology & Evolution*, 34(5), 459–473. <https://doi.org/10.1016/j.tree.2019.01.009>
- Hostetter, N. J., & Royle, J. A. (2020). Movement-assisted localization from acoustic telemetry data. *Movement Ecology*, 8(1), 15. <https://doi.org/10.1186/s40462-020-00199-6>
- Hussey, N. E., Kessel, S. T., Aarestrup, K., Cooke, S. J., Cowley, P. D., Fisk, A. T., Harcourt, R. G., Holland, K. N., Iverson, S. J., Kocik, J. F., Mills Flemming, J. E., & Whoriskey, F. G. (2015). Aquatic animal telemetry: A panoramic window into the underwater world. *Science*, 348(6240), 1255642. <https://doi.org/10.1126/science.1255642>
- Jacoby, D. M. P., & Freeman, R. (2016). Emerging network-based tools in movement ecology. *Trends in Ecology & Evolution*, 31(4), 301–314. <https://doi.org/10.1016/j.tree.2016.01.011>
- Jonsen, I. D., Patterson, T. A., Costa, D. P., Doherty, P. D., Godley, B. J., Grecian, W. J., Guinet, C., Hoenner, X., Kienle, S. S., Robinson, P. W., Votier, S. C., Whiting, S., Witt, M. J., Hindell, M. A., Harcourt, R. G., & McMahon, C. R. (2020). A continuous-time state-space model for rapid quality control of argos locations from animal-borne tags. *Movement Ecology*, 8(1), 31. <https://doi.org/10.1186/s40462-020-00217-7>
- Kessel, S. T., Cooke, S. J., Heupel, M. R., Hussey, N. E., Simpfendorfer, C. A., Vagle, S., & Fisk, A. T. (2014). A review of detection range testing in aquatic passive acoustic telemetry studies. *Reviews in Fish Biology and Fisheries*, 24(1), 199–218. <https://doi.org/10.1007/s11160-013-9328-4>
- Kraft, S., Gandra, M., Lennox, R. J., Mourier, J., Winkler, A. C., & Abecasis, D. (2023). Residency and space use estimation methods based on passive acoustic telemetry data. *Movement Ecology*, 11(1), 12. <https://doi.org/10.1186/s40462-022-00364-z>
- Lavender, E., Aleynik, D., Dodd, J., Illian, J., James, M., Wright, P. J., Smout, S., & Thorburn, J. (2021a). Movement patterns of a critically endangered elasmobranch (*Dipturus intermedius*) in a marine protected area. *Aquatic Conservation: Marine and Freshwater Ecosystems*, 32(2), 348–365. <https://doi.org/10.1002/aqc.3753>
- Lavender, E., Aleynik, D., Dodd, J., Illian, J., James, M., Wright, P. J., Smout, S., & Thorburn, J. (2021b). Environmental cycles and individual variation in the vertical movements of a benthic elasmobranch. *Marine Biology*, 168(11), 164. <https://doi.org/10.1007/s00227-021-03973-1>
- Lavender, E., Biber, S., Illian, J., James, M., Wright, P. J., Thorburn, J., & Smout, S. (2023). An integrative modelling framework for passive acoustic telemetry. *Methods in Ecology and Evolution*, 14(10), 2626–2638. <https://doi.org/10.1111/2041-210X.14193>
- Lavender, E., Scheidegger, A., Albert, C., Biber, S., Aleynik, D., Dodd, J., Cole, G., Wright, P. J., James, M., Illian, J., Smout, S., Thorburn, J., & Moor, H. (2025). Animal tracking with particle algorithms for conservation. *bioRxiv*. <https://doi.org/10.1101/2025.02.13.638042>
- Lavender, E., Scheidegger, A., Albert, C., Biber, S., Illian, J., Thorburn, J., Smout, S., & Moor, H. (2024a). patter: Particle algorithms for animal tracking in R and Julia. *Methods in Ecology and Evolution*. <https://doi.org/10.1101/2024.07.30.605733>
- Lavender, E., Scheidegger, A., Albert, C., Biber, S., Illian, J., Thorburn, J., Smout, S., & Moor, H. (2024b). Particle algorithms for animal movement modelling in receiver arrays (R code) [Dataset]. *Zenodo*. <https://doi.org/10.5281/zenodo.13767598>
- Lea, J. S. E., Humphries, N. E., von Brandis, R. G., Clarke, C. R., & Sims, D. W. (2016). Acoustic telemetry and network analysis reveal the space use of multiple reef predators and enhance marine protected area design. *Proceedings of the Royal Society B: Biological Sciences*, 283(1834), 20160717. <https://doi.org/10.1098/rspb.2016.0717>
- Liu, C., Cowles, G. W., Zemeckis, D. R., Fay, G., Le Bris, A., & Cadrin, S. X. (2019). A hardware-accelerated particle filter for the geolocation of demersal fishes. *Fisheries Research*, 213, 160–171. <https://doi.org/10.1016/j.fishres.2019.01.019>
- Maken, F. A., Ramos, F., & Ott, L. (2022). Stein particle filter for nonlinear, non-gaussian state estimation. *IEEE Robotics and Automation Letters*, 7(2), 5421–5428. <https://doi.org/10.1109/LRA.2022.3153705>
- Matley, J. K., Klinard, N. V., Barbosa Martins, A. P., Aarestrup, K., Aspillaga, E., Cooke, S. J., Cowley, P. D., Heupel, M. R., Lowe, C. G., Lowerre-Barbieri, S. K., Mitamura, H., Moore, J.-S., Simpfendorfer, C. A., Stokesbury, M. J. W., Taylor, M. D., Thorstad, E. B., Vandergoot, C. S., & Fisk, A. T. (2022). Global trends in aquatic animal tracking with acoustic telemetry. *Trends in Ecology & Evolution*, 37(1), 79–94. <https://doi.org/10.1016/j.tree.2021.09.001>
- Matley, J. K., Klinard, N. V., Larocque, S. M., McLean, M. F., Brownscombe, J. W., Raby, G. D., Nguyen, V. M., & Barbosa Martins, A. P. (2023). Making the most of aquatic animal tracking: A review of complementary methods to bolster acoustic telemetry. *Reviews in Fish Biology and Fisheries*, 33(1), 35–54. <https://doi.org/10.1007/s11160-022-09738-3>
- Morales, J. M., Moorcroft, P. R., Matthiopoulos, J., Frair, J. L., Kie, J. G., Powell, R. A., Merrill, E. H., & Haydon, D. T. (2010). Building the bridge between animal movement and population dynamics. *Philosophical Transactions of the Royal Society, B: Biological Sciences*, 365(1550), 2289–2301. <https://doi.org/10.1098/rstb.2010.0082>
- Nathan, R., Getz, W. M., Revilla, E., Holyoak, M., Kadmon, R., Saltz, D., & Smouse, P. E. (2008). A movement ecology paradigm for unifying organismal movement research. *Proceedings of the National*

- Academy of Sciences, 105(49), 19052–19059. <https://doi.org/10.1073/pnas.0800375105>
- Nathan, R., Monk, C. T., Arlinghaus, R., Adam, T., Alós, J., Assaf, M., Baktoft, H., Beardsworth, C. E., Bertram, M. G., Bijleveld, A. I., Brodin, T., Brooks, J. L., Campos-Candela, A., Cooke, S. J., Gjelland, K. Ø., Gupte, P. R., Harel, R., Hellström, G., Jeltsch, F., ... Jarić, I. (2022). Big-data approaches lead to an increased understanding of the ecology of animal movement. *Science*, 375(6582), eabg1780. <https://doi.org/10.1126/science.abg1780>
- Niella, Y., Flávio, H., Smoothery, A. F., Aarestrup, K., Taylor, M. D., Peddemors, V. M., & Harcourt, R. (2020). Refined shortest paths (RSP): Incorporation of topography in space use estimation from node-based telemetry data. *Methods in Ecology and Evolution*, 11(12), 1733–1742. <https://doi.org/10.1111/2041-210X.13484>
- Patterson, T. A., Thomas, L., Wilcox, C., Ovaskainen, O., & Matthiopoulos, J. (2008). State-space models of individual animal movement. *Trends in Ecology & Evolution*, 23(2), 87–94. <https://doi.org/10.1016/j.tree.2007.10.009>
- Pedersen, M. W., Righton, D., Thygesen, U. H., Andersen, K. H., & Madsen, H. (2008). Geolocation of North Sea cod (*Gadus morhua*) using hidden Markov models and behavioural switching. *Canadian Journal of Fisheries and Aquatic Sciences*, 65(11), 2367–2377. <https://doi.org/10.1139/F08-144>
- Pedersen, M. W., & Weng, K. C. (2013). Estimating individual animal movement from observation networks. *Methods in Ecology and Evolution*, 4(10), 920–929. <https://doi.org/10.1111/2041-210X.12086>
- R Core Team. (2023). *R: a language and environment for statistical computing* (version 4.3.1) [Computer software]. R Foundation for Statistical Computing. <https://r-project.org>
- Riotte-Lambert, L., & Matthiopoulos, J. (2020). Environmental predictability as a cause and consequence of animal movement. *Trends in Ecology & Evolution*, 35(2), 163–174. <https://doi.org/10.1016/j.tree.2019.09.009>
- Rutz, C., Loretto, M.-C., Bates, A. E., Davidson, S. C., Duarte, C. M., Jetz, W., Johnson, M., Kato, A., Kays, R., Mueller, T., Primack, R. B., Ropert-Coudert, Y., Tucker, M. A., Wikelski, M., & Cagnacci, F. (2020). COVID-19 lockdown allows researchers to quantify the effects of human activity on wildlife. *Nature Ecology & Evolution*, 4(9), 1156–1159. <https://doi.org/10.1038/s41559-020-1237-z>
- Shaw, A. K. (2020). Causes and consequences of individual variation in animal movement. *Movement Ecology*, 8(1), 12. <https://doi.org/10.1186/s40462-020-0197-x>
- Simpfendorfer, C. A., Heupel, M. R., & Hueter, R. E. (2002). Estimation of short-term centers of activity from an array of omnidirectional hydrophones and its use in studying animal movements. *Canadian Journal of Fisheries and Aquatic Sciences*, 59(1), 23–32. <https://doi.org/10.1139/f01-191>
- Udyawer, V., Dwyer, R. G., Hoenner, X., Babcock, R. C., Brodie, S., Campbell, H. A., Harcourt, R. G., Huveneres, C., Jaine, F. R. A., Simpfendorfer, C. A., Taylor, M. D., & Heupel, M. R. (2018). A standardised framework for analysing animal detections from automated tracking arrays. *Animal Biotelemetry*, 6(1), 17. <https://doi.org/10.1186/s40317-018-0162-2>
- Whoriskey, K., Martins, E. G., Auger-Méthé, M., Gutowsky, L. F. G., Lennox, R. J., Cooke, S. J., Power, M., & Mills Flemming, J. (2019). Current and emerging statistical techniques for aquatic telemetry data: A guide to analysing spatially discrete animal detections. *Methods in Ecology and Evolution*, 10(7), 935–948. <https://doi.org/10.1111/2041-210X.13188>
- Winton, M. V., Kneebone, J., Zemeckis, D. R., & Fay, G. (2018). A spatial point process model to estimate individual centres of activity from passive acoustic telemetry data. *Methods in Ecology and Evolution*, 9(11), 2262–2272. <https://doi.org/10.1111/2041-210X.13080>

## SUPPORTING INFORMATION

Additional supporting information can be found online in the Supporting Information section at the end of this article.

**Figure S1.** True process models for (a) movements and (b) acoustic observations in the two simulated study systems.

**Figure S2.** Simulated array designs.

**Figure S3.** Process models for movements (a–c) and acoustic observations (d–f) in sensitivity analyses.

**Figure S4.** Utilisation distributions (UDs) reconstructed by different algorithms in selected array designs for a hypothetical study system.

**Figure S5.** The distribution of skill metrics in selected arrays for a hypothetical study system.

**Figure S6.** The distribution of skill metrics for two hypothetical study systems across simulated arrays.

**Figure S7.** Wall time for performance simulations.

**Figure S8.** Convergence statistics for sensitivity analyses.

**Figure S9.** Utilisation distributions (UDs) from sensitivity analyses of the movement parameter  $k$ .

**Figure S10.** Utilisation distributions (UDs) from sensitivity analyses of the movement parameter  $\theta$ .

**Figure S11.** Utilisation distributions (UDs) from sensitivity analyses of the movement parameter mobility.

**Figure S12.** Utilisation distributions (UDs) from sensitivity analyses of the acoustic observation process parameter  $\alpha$ .

**Figure S13.** Utilisation distributions (UDs) from sensitivity analyses of the acoustic observation process parameter  $\beta$ .

**Figure S14.** Utilisation distributions (UDs) from sensitivity analyses of the acoustic observation process parameter  $\gamma$ .

**Figure S15.** Algorithm sensitivity to the movement model.

**Figure S16.** Algorithm sensitivity to the acoustic observation model.

**Figure S17.** Mean error for heuristic algorithms versus mis-specified particle algorithms.

**Table S1.** Summary of notation.

**Table S2.** Simulation parameters.

**Table S3.** Simulated array designs.

**Table S4.** Algorithm implementations for ‘performance’ analyses.

**Table S5.** Algorithm implementations for ‘sensitivity’ analyses.

**Data S1.** Supporting Information.

**How to cite this article:** Lavender, E., Scheidegger, A., Albert, C., Biber, S. W., Illian, J., Thorburn, J., Smout, S., & Moor, H. (2025). Particle algorithms for animal movement modelling in receiver arrays. *Methods in Ecology and Evolution*, 00, 1–12. <https://doi.org/10.1111/2041-210X.70028>